Optica Applicata, Vol. LV, No. 1, 2025
DOI: 10.37190/oa/195988

Flexible design of progressive addition lenses for effective sizing of viewing zones using ellipse, hyperbola, parabola, and circle parametric equations

Lefei MA[1], Huazhong XIANG[1,*], Xin ZHANG[1], Hui CHENG[1], Zexi ZHENG[2], Jiabi CHEN[2], Cheng WANG[1], Dawei ZHANG[3,4], Songlin ZHUANG[3,4]

[1]School of Health Science and Engineering, University of Shanghai for Science and Technology, 516 Jun Gong Road, Shanghai 200093, China

[2]School of Mechanical Engineering, University of Shanghai for Science and Technology, Shanghai 200093, China

[3]Engineering Research Center of Optic Instrument and System, Ministry of Education, University of Shanghai for Science and Technology, Shanghai 200093, China

[4]School of Optical-Electrical and Computer Engineering, University of Shanghai for Science and Technology, Shanghai 200093, China

[*]Corresponding author: xiang3845242@163.com

This study addresses the critical issue of optical power distribution in progressive addition lenses (PALs). We introduce a novel approach by defining the addition vertex power curve along the meridian line as a trigonometric function. Four distinct conic equations (ellipse, hyperbola, parabola, and circle) are proposed to extend power distribution evenly across the lens surface. An offset parameter is introduced for controlling viewing area widths. The elliptical equations offer the best results for larger fixed focus areas, while circular equations excel for smaller areas. This personalized method caters to individual patient needs, providing optimized PAL designs.

Keywords: progressive addition lenses, power, eccentricity, astigmatism, optimization.

1. Introduction

Presbyopia refers to the phenomenon where the ability of the eye to adjust diminishes, making it difficult to focus on near objects, typically occurring around the age of forty, affecting approximately a quarter of the global population [1,2]. In the Asia-Pacific region and Eastern Europe, with the promotion of optometric education centered around

progressive lens fitting, an increasing number of people are considering progressive addition lenses (PALs) as an important option for vision correction [3,4]. PALs are lenses where the optical power gradually increases as the user's eye moves from far to near and from top to bottom, ensuring clear vision for both distance and near vision [5-8].

Currently, the design methods for PALs mainly involve direct and indirect approaches [5]. WINTHROP [9], BAUDART [10], and others have used the direct method to design PALs, where they first determine the optical powers and center points of the distance and near vision areas, connect the midpoint to obtain a meridian line, then determine the curvature radius variation along the meridian line points, and generate the entire surface's sagittal distribution directly by specifying curves intersecting the meridian line. The indirect method involves constructing a cost function based on the difference between mean curvature and principal curvature, minimizing it by solving differential equations to complete the lens design [11,12]. WANG *et al*. [13] utilized the variational finite difference method to minimize the cost function and design PALs accordingly. This method can produce lenses satisfactory to optical engineers within seconds. TAZEROUALTI [14] and MENDIOLA-ANDA [15] explored additional approaches to improve the convergence or smoothness of the final solution by incorporating more terms into the merit function for peripheral power distributions. Nonetheless, the minimization of such a function poses problems unless suitable weight functions are selected [16]. In recent years, there have been advancements in the direct method for designing progressive multifocal lenses. In 2014, TANG *et al*. [17] proposed using genetic algorithms to find optimal meridian designs for PALs; in 2017, LU *et al*. [18] proposed a design approach for the meridian optical power of PALs using involutes; in 2022, ZHANG *et al*. [19] proposed a method for dual-fitting design of progressive multifocal lens meridians. This method adopts two polynomial curves to fit the meridians from the far vision point and the near vision point of the lens, obtaining the meridian focal power that meets the design requirements.

From the above, it can be seen that current optimization of the direct method for designing PALs mainly focuses on the variation of optical power along the meridian, while there is relatively little research on obtaining reasonable optical power contour distributions on the lens surface. Therefore, finding a suitable optical power contour function to optimize the optical performance of progressive lenses is crucial. Hence, building upon existing research [4,12,13], this paper first sets the curvature variation along the meridian to satisfy trigonometric functions, then redesigns the optical power contour distribution of the lens by introducing the equations of conic sections intersecting with cylindrical surfaces. By defining the optical power contour of the lens, controlling the size of the distance and near vision areas, substituting the optical power contour line function into the sagittal equation, the entire surface shape is obtained.

2. Principle of optimal design method

PALs feature a surface with varying curvature, enabling the lens to provide variable optical power for different viewing areas. The distribution of mean curvature along

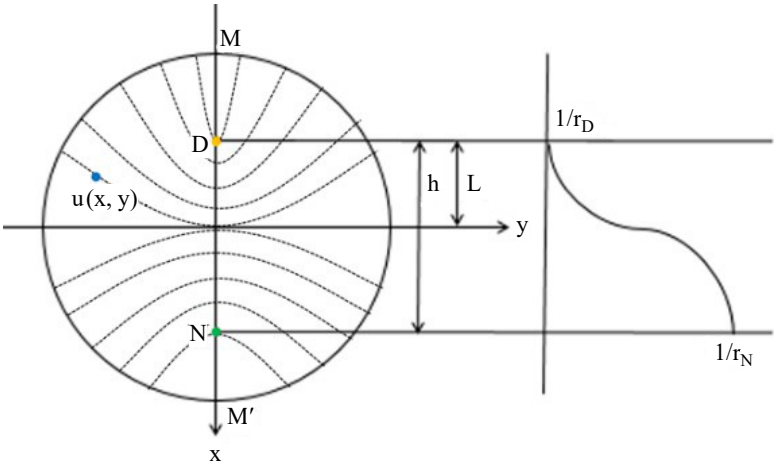

Fig. 1. Schematic of the progressive surface structure.

the lens's meridian significantly impacts the curvature and astigmatism distribution across the entire lens surface. As depicted in Fig. 1, points D and N represent the distance and near reference points, respectively, while MM′ represents the principal vertical meridian line. The change in vertex power along the meridian line is referred to as the addition power curve. To ensure a seamless and continuous visual experience, the design of the meridian line must ensure stable optical effects around points D and N and ensure a smooth and gradual change in the power addition curve $u(x, y)$ across the entire power-adding range. To fulfill these conditions, the curvature of the surface along the meridian line was changed as smoothly as possible. As a criterion for this smoothness, the mean square gradient of $u(x, y)$ must reach the minimal value and satisfy the two-dimensional Laplace equation:

$$\frac{\partial^2 u}{\partial x^2} + \frac{\partial^2 u}{\partial y^2} = 0 \tag{1}$$

To ensure a gradual change in the curvature at the D and N points, the order of the first nonzero order derivative should be as high as possible. We solve Eq. (1) considering the boundary conditions:

$$\begin{cases} u(x, 0) = -L & \text{where} \quad x < -L \\ u(x, 0) = h - L & \text{where} \quad x > h - L \end{cases} \tag{2}$$

Here, h is the distance between points D and N, and L is the distance of point D above origin O. The meridional power law is as follows [9]:

$$\frac{1}{r(u)} = \frac{1}{r_D} + \left(\frac{1}{r_N} - \frac{1}{r_D}\right) C(u) \tag{3}$$

where r_D and r_N are the mean curvature of the distance point D and near point N, respectively. $C(u)$ is a trigonometric function:

$$C(u) = \sin^2\left(\frac{\pi}{2}\frac{-L-u}{-h}\right) \tag{4}$$

After determining the vertex power distribution along the meridian line, the next step involves extending this acquired power distribution to cover the entire lens surface and subsequently calculating the surface height, guided by the principles of differential geometry.

2.1. Design of lens optical power contour

Various methods exist for extending the power distribution along the meridian to cover the entire lens surface. Typically, a contour line of equal power, perpendicular to the meridian line, is selected. These contour lines can take various forms, such as straight lines, circles, hyperbolas, and ellipses.

Figure 2 represents a cross-sectional diagram of a conic surface, where the vertex of the ρoz plane is situated at the origin, and the curvature radius r_i of the conical section is defined as follows [20]:

$$\rho^2 + (1 + k_i)z_1^2 - 2r_i z_i = 0 \tag{5}$$

where k_i is the conic coefficient that determines the type of conic, ρ is the polar coordinate, that is $\rho^2 = x^2 + y^2$, and z is the sag of the surface (the height difference of the z axis). As shown in Fig. 2, when $k_1 < -1$, the conic surface is a hyperbola; when

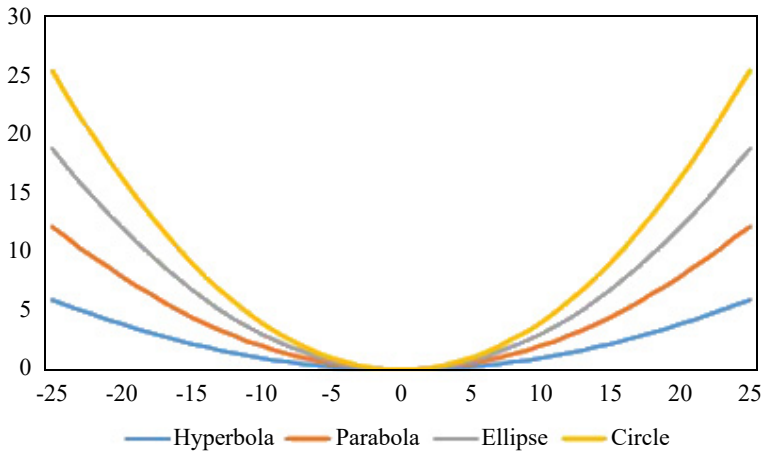

Fig. 2. Cross-section diagram of the conic surface.

$k_2 = -1$, the conic surface is a parabola; when $k_3 > -1$, the conic surface is an ellipse; when $k_4 = 0$, the conic surface is a circle. The generalized Eq. (5) in an XOY coordinate system is

$$y^2 + (1 + k_i)x^2 - 2r_i x = 0 \tag{6}$$

According to $u(x, 0) = x$, and Eq. (6) can be extended to the design of the optical power contour distribution of the lens:

$$y^2 + (1 + k_i)(x - u)^2 - 2r_i(x - u) = 0 \tag{7}$$

Therefore, according to different definitions of the conic curves, the expressions k_i and r_i can be obtained and substituted into Eq. (7). The $u(x, y)$ function solution corresponding to $x \geq 0$ can be solved first; the $u(x, y)$ function solution corresponding to $x < 0$ is solved as

$$y^2 + (k + 1)\Big[|x| - u(x, y)\Big]^2 - 2r_1\Big[|x| - u(x, y)\Big] = 0 \tag{8}$$

2.2. Design of different optical power contours

2.2.1. Optical power contour design based on hyperbola

According to Eq. (8), the hyperbola equation is

$$\begin{cases} \dfrac{\Big[|x| - u - a_1\Big]^2}{a_1^2} - \dfrac{y^2}{b_1^2} = 1 \\ a_1^2 = \dfrac{r_1^2}{(1 + k_1)^2} \\ b_1^2 = -\dfrac{r_1^2}{1 + k_1} \end{cases} \tag{9}$$

For $a_2 > 0$ and $b_2 > 0$, then $k_1 > -1$. According to hyperbolic properties, the larger the hyperbolic eccentricity e_1, the larger is the opening. When $x \geq 0$, the eccentricity should decrease with an increase in u. The eccentricity can be expressed as follows:

$$e_1 = \sqrt{-k_1} = \frac{h}{u} \tag{10}$$

For the hyperbola, when $x \geq 0$, the larger $u(x, y)$ is, the smaller the opening of the hyperbola should be; thus, $u(x, y)$ is directly proportional to b_1. Let

$$\begin{cases} b_1^2 = \dfrac{-r_1^2}{1+k_1} = q_1 u, & q_1 > 0 \\ r_1 = q_1 \dfrac{h^2 - u^2}{u}, & q_1 > 0 \end{cases} \tag{11}$$

where q_1 is the parameter that sets the distribution size of the optical power contour in the focal area of the lens in the distance and near zones.

2.2.2. Optical power contour design based on parabola

According to Eq. (8), the parabolic equation is set as follows:

$$y^2 + (1+k_2)\left(|x| - u\right)^2 - a_2\left(|x| - u\right) = 0 \tag{12}$$

where $a_2 = 2r_2$, and $k_2 = -1$. The larger a_2 is, the smaller the opening of the parabola. When $x \geq 0$, the opening size of the parabola decreases with an increase in u. Let

$$r_2 = q_2 \frac{h^2 - u^2}{u}, \quad q_2 > 1 \tag{13}$$

where q_2 is the parameter that sets the distribution size of the optical power contour in the focal area of the lens in the distance and near zones.

2.2.3. Optical power contour design based on ellipse

According to Eq. (8), the elliptic equation is set as follows:

$$\begin{cases} \dfrac{y^2}{b_3^2} + \dfrac{\left[|x| - u - a_3\right]^2}{a_3^2} = 1 \\ a_3^2 = \dfrac{r_3^2}{(1+k_3)^2} \\ b_3^2 = \dfrac{r_3^2}{1+k_3} \end{cases}, \quad a_3 > b_3 > 0 \tag{14}$$

If $a_3 > b_3 > 0$, then $-1 < k_3 < 0$. When $x \geq 0$, the larger the heart rate e_3 of the ellipse, the flatter the ellipse. The eccentricity should increase with an increase in u; therefore, the eccentricity is expressed as follows:

$$e_3 = \sqrt{\frac{a_3^2 - b_3^2}{a_3^2}} = \sqrt{-k_3} = \sqrt{\frac{u}{h}} \tag{15}$$

When $x \geq 0$, and a_3 should decrease with an increase in u, and $a_3 > 0$, such that

$$a_3^2 = \frac{r_3^2}{(1+k_3)^2} = \left(\frac{r_3 h}{h-u}\right)^2 \geq q_3^2(h-u)^2, \qquad q_3 > 0 \tag{16}$$

Accordingly,

$$r_3 \geq q_3 \frac{(h-u)^2}{h} \tag{17}$$

because

$$\begin{cases} \dfrac{(h-u)^2}{h} = \dfrac{h^2-2hu+u^2}{h} \leq \dfrac{h^2-2u^2+u^2}{u} = \dfrac{(h-u)^2}{u} \\ r_3 = q_3 \dfrac{h^2-u^2}{h} \end{cases} \tag{18}$$

where q_3 is the parameter that sets the distribution size of the optical power contour in the focal area of the lens in the distance and near zones.

2.2.4. Optical power contour design based on circle

According to Eq. (8), the deformation of the circle equation is set as follows:

$$y^2 + (k_4+1)\Big(|x|-u\Big)^2 - 2r_4\Big(|x|-u\Big) = 0 \tag{19}$$

where $1 + k_4 = 1$, that is, $k_4 = 0$. When $x \geq 0$, the larger r_4 is, the larger is the circle. The circle decreases with an increase in u, and $r_4 > h - u$; let

$$\begin{cases} r_4 = q_4 \dfrac{h^2-u^2}{u} \\ q_4 \dfrac{h^2-u^2}{u} \geq \dfrac{2q_4(h-u)\sqrt{hu}}{u} \geq 2q_4(h-u) \end{cases} \tag{20}$$

where q_4 is the parameter that sets the distribution size of the optical power contour in the focal area of the lens in the distance and near zones.

To define the range size of the distance and near zone, let $u(x + \Delta x_i, y)$, $i = 1, 2, 3, 4$. As shown in Fig. 3(a), this method is used to solve the contour line of one of the unfixed foci when the contour distribution of optical foci is circular. Figure 3(b) shows the contour distribution curve of the optical focal power after Δx_4 of downward movement.

To ensure that the channel length remains unchanged after movement, it can be expressed as follows:

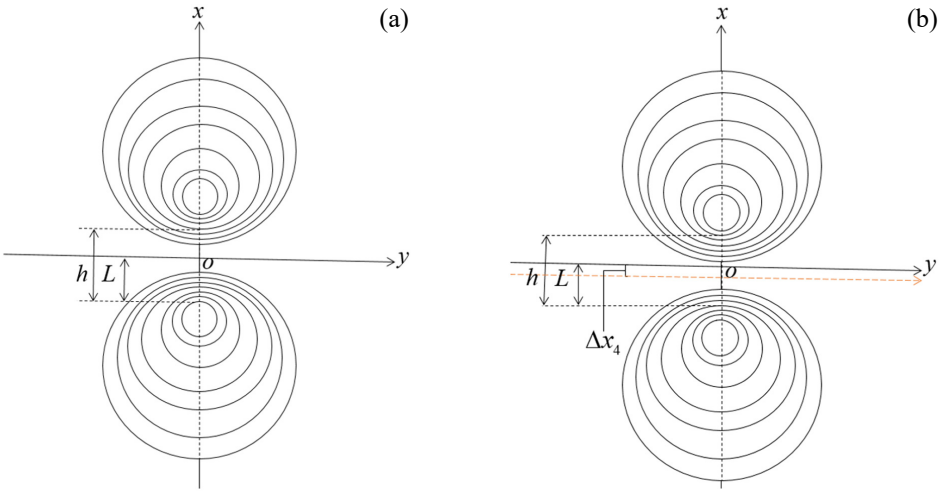

Fig. 3. Circular distribution $u(x, y)$ contour distribution. (a) Downward and forward movement. (b) Downward movement.

$$y^2 + \left\{ |x - \Delta x_4| - \left[u(x, y) - \Delta x_4 \right] \right\}^2 - 2q_4 \frac{h^2 - u^2(x, y)}{u(x, y)} \left\{ |x - \Delta x_4| - \left[u(x, y) - \Delta x_4 \right] \right\} = 0 \tag{21}$$

We assume that $x = L - p$ is the horizontal coordinate of the near reference point, and $x = h - L + p$ is the horizontal coordinate of the distant reference point. When $x = h - L + p$ and $u = h - L$, the area width of the reference point astigmatism less than 0.5 D is W_N. For $x = L - p$ and $u = L$, the width of the lateral visual area with the reference point astigmatism less than 0.5 D is W_D. Substituting these values, the following is obtained:

$$\begin{cases} \left(\dfrac{W_N}{2} \right)^2 + p^2 - 2q_4 p \dfrac{h^2 - (h - L - \Delta x_4)^2}{h - L - \Delta x_4} = 0 \\ \left(\dfrac{W_D}{2} \right)^2 + p^2 - 2q_4 p \dfrac{h^2 - (L - \Delta x_4)^2}{L - \Delta x_4} = 0 \end{cases} \tag{22}$$

When entering h, L, p, W_N, and W_D, the values of q_4 and Δx_4 can be obtained using Eq. (22). When $x - \Delta x_4 \geq 0$, the parameters are substituted into Eq. (21) to obtain $u(x, y)$. When $x - \Delta x_4 < 0$, $u(x, y) = -u(|x|, y) - 2\Delta x_4$. Similarly, the optical power contour distribution of the other three conic curves can be obtained to define the viewing area width of the reference point of the near and distance area.

3. Results and discussion

3.1. Optical parameters and simulations

To render the astigmatic gradient change in the visual distance region more compatible and comfortable for the human eye, two different width ranges W_D ($W_{D1} = 24$, $W_{D2} = 40$) were used for flexible design. The optical parameters required for the PALs are summarized in Table 1.

T a b l e 1. Design parameters of four sets of progressive addition lenses.

Case	SPH [D]	ADD [D]	F [D]	n	h [mm]	L [mm]	p [mm]	W_N [mm]	W_D [mm]	CT [mm]
PAL	0	2	4	1.56	14	2	4	12	24	2.3
	0	2	4	1.56	14	2	4	12	40	2.3

SPH: sphere, ADD: addition power, CT: central thickness, F: front surface power with a refractive index $n = 1.552$.

Four groups of lenses based on hyperbola, parabola, ellipse, and circle equation are calculated using the above parameters, as shown in Fig. 4, and it is based on the contour of the function $u(x, y)$ solved in the second part of $\{x, y \mid x^2 + y^2 \leq 25^2\}$.

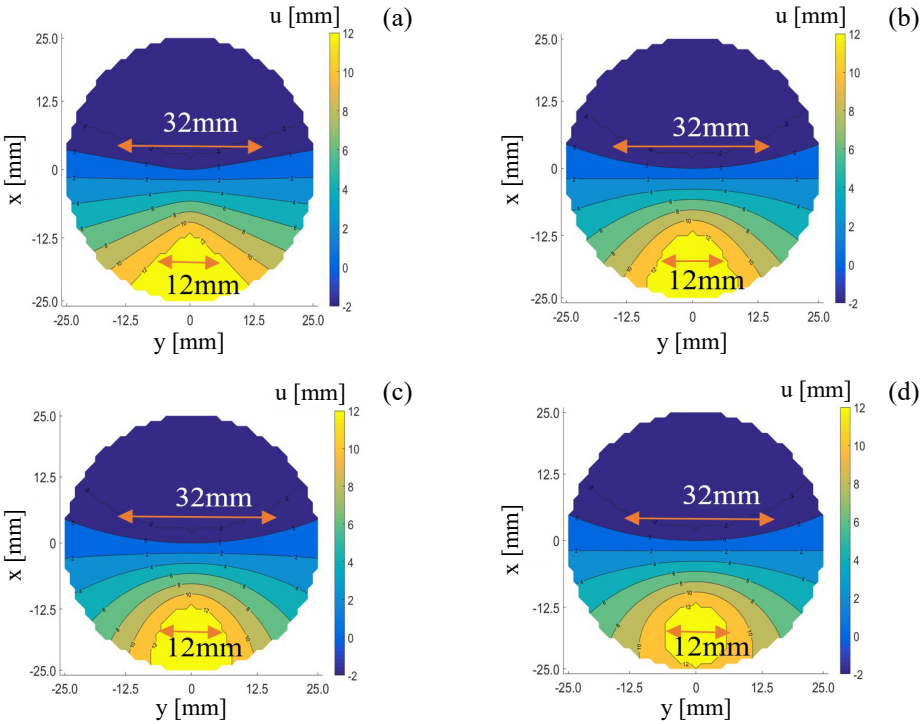

Fig. 4. Contour $u(x, y)$ obtained by solving different conic curve equations. (a) hyperbola, (b) parabola, (c) ellipse, and (d) circle.

The results are depicted in Fig. 4(a), (b), (c), and (d), with W_N = 12 mm and W_D = = 32 mm. The simulations for each case were conducted using the free-form verifier (FFV) software developed by ROTLEX in Israel. This commercial software functions as a Moiré deflectometer employing a point source. It generates mean curvature distributions by superimposing two pitch gratings with different angles. In the ROTLEX system, the angle between the interfering gratings remains constant. The frequency and orientation of the resulting fringes are highly sensitive to variations in the two pitch values 17. The observation window used exhibited a diameter of 50 mm, significantly larger than a typical spectacle frame. The power distributions observed align with the anticipated outcomes in the viewing zones for each simulation, as shown in Fig. 5.

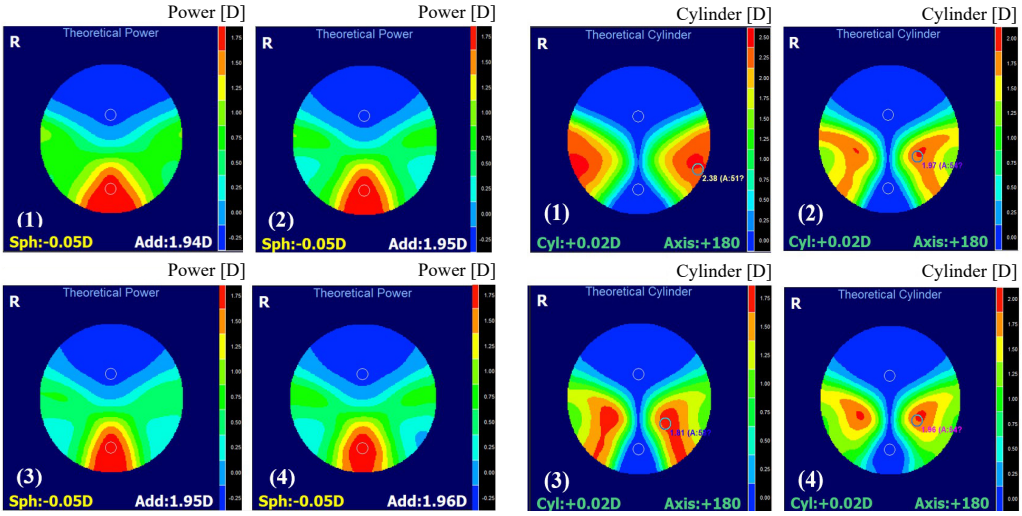

Fig. 5. Simulation of the sphere and cylinder for the two tested PALs: (a) spherical power (1 – hyperbola, 2 – parabola, 3 – ellipse, 4 – circle), and (b) cylinder (1 – hyperbola, 2 – parabola, 3 – ellipse, 4 – circle).

In Fig. 5, the small white circles situated in the distance and near regions represent the distance reference point (0 mm, 8 mm) and the near reference point (2 mm, −16 mm), respectively.

Analyzing the simulation results, the SPH values for the distance zone corresponding to lenses 1–4 are −0.05, −0.05, 0.02, and 0.02 D, respectively. Additionally, the ADD values for these lenses are 1.94, 1.95, 1.95, and 1.96 D, respectively, with a maximum difference of 0.06 D from the theoretical values. These results are in line with the national standard (GB10810.1-2005) [18]. Furthermore, the clear visual range of the near area for lens 1 is larger than that of the other three groups of lenses. Additionally, the contour change in optical power for lenses 2, 3 and 4 is slower relative to that for lens 1. Consequently, the optical power contour distribution of progressive addition free-form surfaces can be tailored based on various conic curves.

3.2. Optical properties analysis

The manufacturing process for the posterior surface of PALs involves the utilization of the CNC optical generating machine Satisloh VFT-orbit, provided by Jiangsu Mingyue Photoelectric Technology Co. Ltd. This machine is employed for operations such as turning, milling, grinding, and polishing.

Subsequently, the lenses undergo inspection using a Visionix VM-2500 Lens Power Mapper. The contour plots illustrating the average spherical power and cylinder (astigmatism) for all tested lenses are presented in Fig. 6. These contour lines are spaced at intervals of 0.25 D for the eight tested lenses. The lenses exhibit a diameter of 50 mm. The surface shape results pertaining to optical power and astigmatism for the four lenses are shown in Fig. 6.

All PAL measurements were acquired by a NIDEK LM-1800P focimeter. The results are shown in Table 2.

By combining the results from Figs. 5 and 6, and Table 2, the maximum difference between the actual distance zone sphere (SPH) of lenses 1 and 4, and the theoretical value can be found to be 0.04 D. The difference between ADD and the theoretical value is 0.05 D. These differences conform to the national standard (GB10810.1-2005).

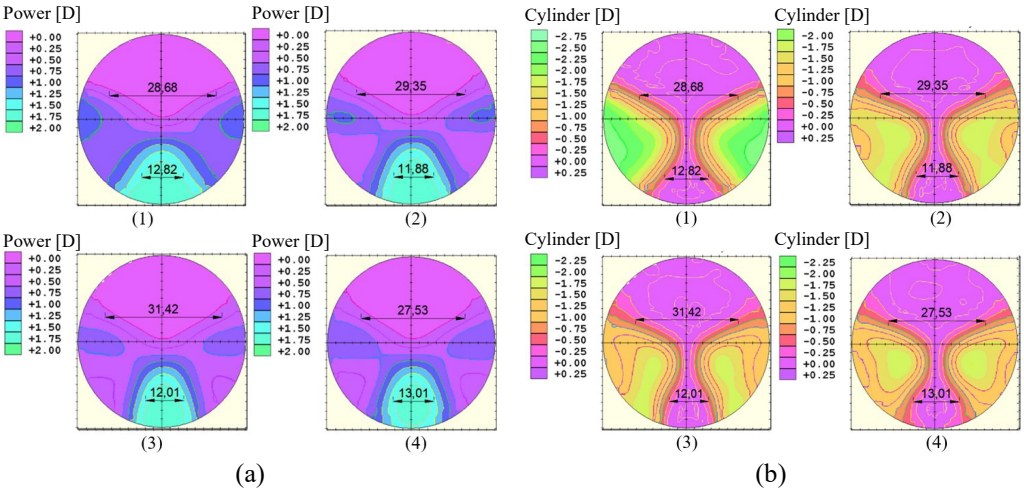

Fig. 6. Contour plots of the four free-form PALs for the different power distribution and cylinder distribution. (a) power (1 – hyperbola, 2 – parabola, 3 – ellipse, 4 – circle), and (b) cylinder (1 – hyperbola, 2 – parabola, 3 – ellipse, 4 – circle).

T a b l e 2. Actual measurement results of four sets of progressive addition lenses.

	Distance SPH [D]	ADD [D]	Actual W_{iD} [mm]	Actual W_{iN} [mm]
Lens 1 (hyperbola)	0.04	1.96	28.68	12.82
Lens 2 (parabola)	0.03	1.95	29.35	11.88
Lens 3 (ellipse)	0.03	1.98	31.42	12.01
Lens 4 (circle)	0.02	1.96	27.53	13.01

The smaller values observed in the four sets of lenses W_D and W_N are smaller than the theoretical value, namely lens 1, lens 2, lens 3, and lens 4, and can be attributed to the distortion inherent in the gradual transition from the inner progressive addition lens to the periphery of the fixed focus region. Regarding astigmatism, the maximum astigmatism of lenses 2, 3, and 4 is less than one times ADD, indicating suitable visual performance. Conversely, lens 1 exhibits a maximum astigmatism of 1.36 times ADD, with greater peripheral astigmatism and relatively inferior visual performance. The order of the values of W_D for the four groups of lenses in descending order is lens 3 > lens 2 > lens 1 > lens 4, and for the values of W_N, the order is lens 4 > lens 1 > lens 3 > lens 2 in descending order. The peripheral distortion of the fixed focus region of the lens calculated by the elliptic equation is small, and the regions with astigmatism greater than 1.75 D for the four groups of lenses are as follows: lens 1 > lens 3 > lens 4 > lens 2. The summation of W_D and W_N for lens 3 is most consistent with the set value. The maximum astigmatism around lens 2 is the smallest, and the ratio of peripheral maximum astigmatism to ADD is the smallest. The area where the peripheral astigmatism of lens 1 is greater than 1.75 D is relatively small.

4. Conclusion

In this research, a novel approach for designing PALs was proposed. The method involved using conic parametric equations to define contour lines of equal power that are perpendicular to the meridian line and extend the power distribution across the entire lens surface. This direct approach aimed to ensure a seamless and continuous visual experience while reducing peripheral astigmatism. The curvature along the meridian of the PAL followed a trigonometric function, and the power distribution was determined based on parameter equations for circles, hyperbolas, parabolas, and ellipses. Four distinct types of PALs were designed, simulated, manufactured, and evaluated using commercial software, with a focus on analyzing the impact of the different conic parametric equations on the optical properties of PALs.

Through a comprehensive investigation involving theoretical analysis, practical processing, testing, and comparative analysis, the study revealed that the choice of conic equation had a notable impact on PAL design. Specifically, PALs designed with the hyperbolic equation exhibited significant peripheral astigmatism that could lead to discomfort and vertigo for wearers. Conversely, PALs calculated using elliptical, circular, and parabolic equations demonstrated lower astigmatism levels. Future research could build upon this design method by transitioning from a spherical inner surface to an aspherical one, thereby further optimizing the PALs to reduce tangential errors and enhance accuracy in real-world outcomes.

References

[1] STOKES J., SHIRNESHAN E., GRAHAM C.A., PAULICH M., JOHNSON N., *Exploring the experience of living with and managing presbyopia*, Optometry and Vision Science **99**(8), 2022: 635-644. https://doi.org/10.1097/opx.0000000000001913

[2] Katz J.A., Karpecki P.M., Dorca A., Chiva-Razavi S., Floyd H., Barnes E., Wuttke M., Donnenfeld E., *Presbyopia – A review of current treatment options and emerging therapies*, Clinical Ophthalmology **15**, 2021: 2167-2178. https://doi.org/10.2147/opth.s259011
[3] Elmadina A.M., *Progressive addition lenses wearers' visual satisfaction among Saudi population*, African Vision and Eye Health **81**(1), 2022: a733. https://doi.org/10.4102/aveh.v81i1.733
[4] Chamorro E., Cleva J.M., Concepción P., Subero M.S., Alonso J., *Lens design techniques to improve satisfaction in free-form progressive addition lens users*, JOJ Ophthalmology **6**(3), 2018: 555688. https://doi.org/10.19080/JOJO.2018.06.555688
[5] Rolland J.P., Davies M.A., Suleski T.J., Evans C., Bauer A., Lambropoulos J.C., Falaggis K., *Freeform optics for imaging*, Optica **8**(2), 2021: 161-176. https://doi.org/10.1364/OPTICA.413762
[6] Jalie M., *Modern spectacle lens design*, Clinical and Experimental Optometry **103**(1), 2020: 3-10. https://doi.org/10.1111/cxo.12930
[7] Legras R., Vincent M., Marin G., *Does visual acuity predict visual preference in progressive addition lenses?*, Journal of Optometry 16(2), 2023: 91-99. https://doi.org/10.1016/j.optom.2022.04.003
[8] Ferrer-Altabás S., Picazo-Bueno J.A., Granero-Montagud L., Micó V., *Shadowfocimetry: Adapting the holographic principle to a manual focimeter for visualization/marking of permanent engravings in progressive addition lenses*, Optics Letters **47**(9), 2022: 2298-2301. https://doi.org/10.1364/OL.454962
[9] Winthrop J.T., *Progressive Addition Spectacle Lens*, United States Patent US4861153, 1989.
[10] Baudart T, *Multifocal Ophthalmic Lens*, United States Patent US6102544, 2000.
[11] Concepción P., Cleva J., Chamorro E., Crespo D., García M., Gago C., Subero M., Alonso J., *Clinical evaluation of free-form PALs: Customized vs standard designs*, European Academy of Optometry and Optics Annual Conference, Barcelona, Spain, 2017: 34-36.
[12] Loos J., Greiner G., Seidel H.P., *A variational approach to progressive lens design*, Computer-Aided Design **30**(8), 1998: 595-602. https://doi.org/10.1016/S0010-4485(97)00102-4
[13] Wang J., Santosa F., *A numerical method for progressive lens design*, Mathematical Models and Methods in Applied Sciences **14**(4) 2004: 619-640. https://doi.org/10.1142/S0218202504003386
[14] Tazeroualti M., *Designing a progressive lens*, [In] *Curves and Surfaces in Geometric Design*, AK Peters, 1994: 467-474.
[15] Mendiola-Anda G., *Design of Surfaces under Physical Constraints and its Application to the Design of Ophthalmic Lenses*, Ph.D. Dissertation, School of Computing Sciences, University of East Anglia, Norwich, England, 2006.
[16] Barbero S., del Mar González M., *Admissible surfaces in progressive addition lenses*, Optics Letters **45**(20), 2020: 5656-5659. https://doi.org/10.1364/OL.401927
[17] Tang Y.H., Wu Q.Y., Chen X.Y., Zhang H., Wu Y.L., *Optimization design of the meridian line of progressive addition lenses based on genetic algorithm*, Acta Optica Sinica **34**(9), 2014: 922005. https://doi.org/10.3788/aos201434.0922005
[18] Lu H.Y., Bai D.F., Ma J.W., *Design for initial vector height model of progressive addition lenses surface*, Laser and Optoelectronics Progress **54**(3), 2017: 32201. https://doi.org/10.3788/lop54.032201
[19] Zhang H.X., Wu Q.Y., Tang Y.H., Lv X.Z., Chen X.Y., Hou Y.W., *Bi-directional fitting design of meridian lines for progressive addition lenses*, Infrared and Laser Engineering **51**(6), 2022: 20210630.
[20] Guggenheimer H.W., *Differential Geometry*, Courier Corporation, 2012.

Received September 28, 2024
in revised form November 11, 2024